Cell Reports
Report

Slit/Robo Signaling Regulates Cell Fate Decisions in the Intestinal Stem Cell Lineage of *Drosophila*

Benoît Biteau[1,*] and Heinrich Jasper[2]
[1]Department of Biomedical Genetics, University of Rochester Medical Center, 601 Elmwood Avenue, Rochester, NY 14642, USA
[2]Buck Institute for Research on Aging, 8001 Redwood Boulevard, Novato, CA 94945, USA
*Correspondence: benoit_biteau@urmc.rochester.edu
http://dx.doi.org/10.1016/j.celrep.2014.05.024

SUMMARY

In order to maintain tissue homeostasis, cell fate decisions within stem cell lineages have to respond to the needs of the tissue. This coordination of lineage choices with regenerative demand remains poorly characterized. Here, we identify a signal from enteroendocrine cells (EEs) that controls lineage specification in the *Drosophila* intestine. We find that EEs secrete Slit, a ligand for the Robo2 receptor in intestinal stem cells (ISCs) that limits ISC commitment to the endocrine lineage, establishing negative feedback control of EE regeneration. Furthermore, we show that this lineage decision is made within ISCs and requires induction of the transcription factor Prospero in ISCs. Our work identifies a function for the conserved Slit/Robo pathway in the regulation of adult stem cells, establishing negative feedback control of ISC lineage specification as a critical strategy to preserve tissue homeostasis. Our results further amend the current understanding of cell fate commitment within the *Drosophila* ISC lineage.

INTRODUCTION

Whereas determinants of lineage specification in several somatic stem cell lineages of vertebrate model systems have been identified (Beck and Blanpain, 2012; Rock and Hogan, 2011; Yeung et al., 2011), little is known about how tissue needs are monitored and information about specific missing cell types is relayed to stem cells. The *Drosophila* posterior midgut has emerged as a powerful genetically tractable system for the characterization of stem cell function and the control of epithelial homeostasis, serving as an ideal model for the identification of such signaling interactions (Biteau et al., 2011; Casali and Batlle, 2009; Jiang and Edgar, 2012; Wang and Hou, 2010). Intestinal stem cells (ISCs) can regenerate all cell types of the intestinal epithelium, producing, through asymmetric and symmetric divisions, precursor cells (such as enteroblasts [EBs]) that differentiate into either enterocytes (ECs) or enteroendocrine cells (EEs) (de Navascués et al., 2012; Micchelli and Perrimon, 2006; Ohlstein and Spradling, 2006, 2007).

Homeostasis of the intestinal epithelium is maintained both by cell-autonomous control of proliferation and differentiation in the ISC lineage as well as by cell-cell interactions. One example is the induction of ISC proliferation by damaged ECs, a mechanism that allows regenerating new ECs as needed (Amcheslavsky et al., 2009; Buchon et al., 2009; Chatterjee and Ip, 2009; Cronin et al., 2009; Jiang et al., 2009). So far, it remained unclear if EEs have a similar ability to control the regeneration of their own lineage. The balance between EC and EE differentiation is influenced by Notch signaling. High expression of the Delta ligand in ISCs activates Notch in EBs, promoting EC differentiation. Low-Delta-expressing ISCs, on the other hand, promote the differentiation of their daughter cells into EEs (Ohlstein and Spradling, 2007). However, the signals that control ISC cell fate decisions or regulate the level of Delta expression in ISCs have not been identified to date.

Here, we report the identification of Slit/Robo2 signaling as a critical regulator of the balance between the EE and EC lineages. We show that the Slit ligand is expressed in EEs, establishing a retrograde signal that controls cell fate decisions in ISCs. Our results suggest that Robo2 regulates lineage specification by inhibiting the expression of the transcription factor Prospero in ISCs prior to cell division, acting upstream of the establishment of differential Notch signaling.

RESULTS AND DISCUSSION

Slit/Robo Signaling between Enteroendocrine and Progenitor Cells in the Posterior Midgut

In a screen for new signaling molecules involved in the regulation of tissue homeostasis in the posterior midgut, we identified the secreted ligand Slit as a factor specifically expressed in EEs. Using a LacZ-expressing reporter line inserted in the *slit* locus ($Slit^{PZ05248}$), we found that the Slit promoter is active in a subset of cells in the intestinal epithelium (Figure S1A) and that these cells represent Prospero-positive EEs (Figure 1A), but not small esg-positive ISCs/EBs or polyploid ECs (Figure 1B). Immunocytochemistry confirmed that high levels of Slit protein are present in the cytoplasm of Prospero-positive and esg-negative diploid EEs (Figures 1C, 1D, and S1B). Interestingly, the Slit protein can also be detected on escargot-positive ISCs and EBs (Figures 1D and S1C), suggesting that this secreted molecule diffuses from EEs to these progenitors.

In *Drosophila*, three Roundabout receptors (Robo1, Robo2/leak, and Robo3) have been shown to transduce the Slit signal

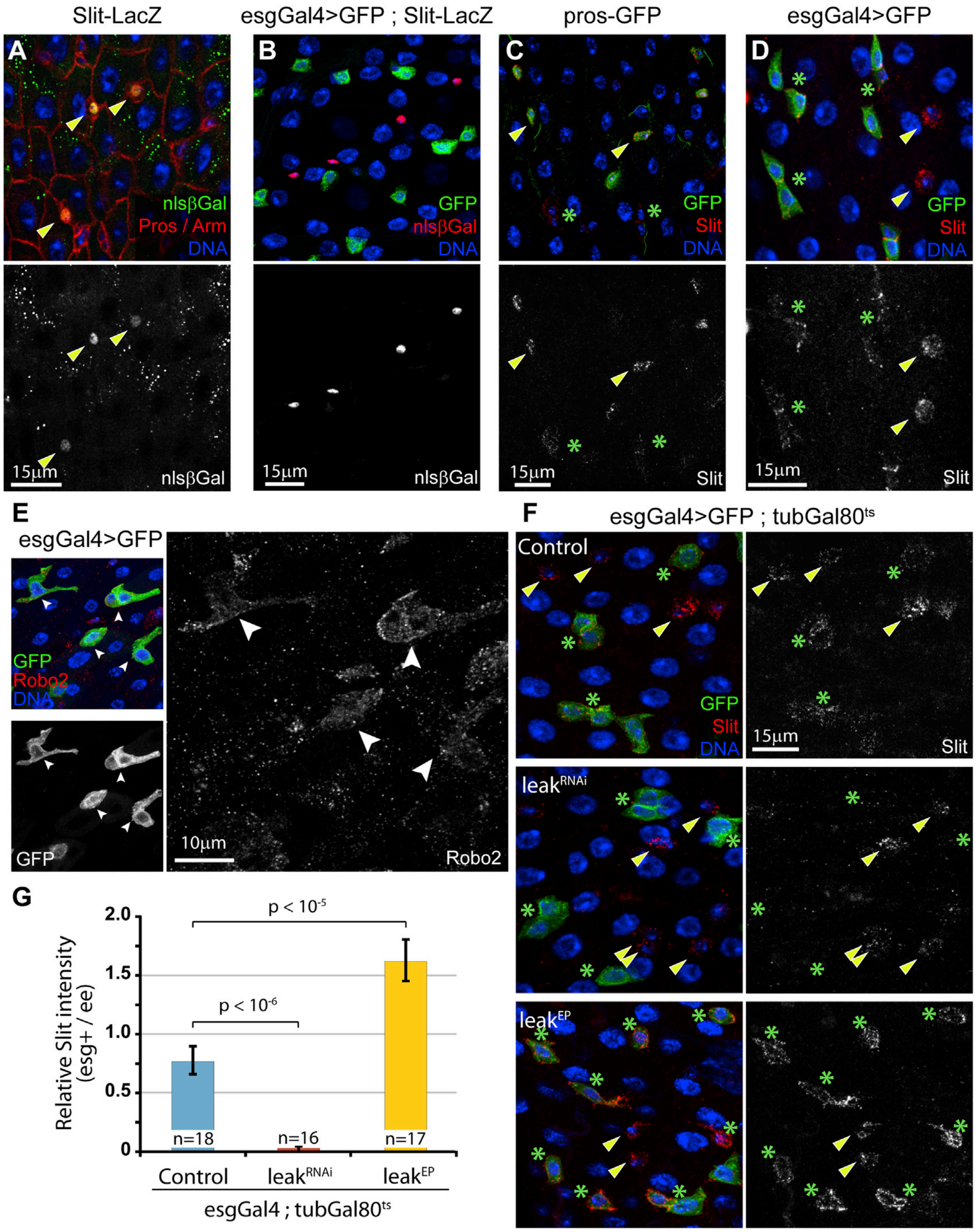

Figure 1. Slit/Robo2 Signaling between Enteroendocrine and Stem/Progenitor Cells in the Posterior Midgut

(A and B) The Slit promoter is active in EEs, as shown by the detection of β-galactosidase in Prospero-positive cells, using the Slit^{PZ05248}-LacZ reporter line (A; arrowheads), and inactive in escargot-positive progenitors and polyploid enterocytes (B).

(C and D) The Slit protein is detected in the cytoplasm of Prospero-GFP-positive cells (C; arrowheads; see Figure S2B for the characterization of the pros-GFP reporter) and at the periphery of escargot-positive cells (D; asterisks).

(E) The Robo2 receptor is expressed in esg-positive cells, as shown by immunocytochemistry using a Robo2-specific antibody.

(F) Knockdown of lea/Robo2 in esg-positive cells is sufficient to abolish the accumulation of Slit at the surface of these cells (asterisks) without affecting Slit expression in EEs (arrowheads). Overexpressing Robo2, using the lea^{EP} line, increases the signal at the periphery of ISCs.

(G) Quantification of Slit immunostaining intensity in esg-positive ISCs/EBs compared to esg-negative diploid EEs in similar conditions as Figure 1F.

n represents the number of pairs of diploid cells (one esg-positive and one esg-negative) that were analyzed. p value from two-tailed Student's t test. Values are presented as average ± SEM. See also Figure S1.

in different biological contexts (Ypsilanti et al., 2010). To determine whether one of these is a receptor for EE-derived Slit, we first assessed whether they are expressed in the intestine. Using genome-wide transcriptome profiling by RNA sequencing, we found that only Robo1 and leak/Robo2 transcripts can be detected in dissected intestines (data not shown). Using previously described antibodies (Kidd et al., 1998; Rajagopalan et al., 2000; Simpson et al., 2000), we further found no evidence that Robo1 and Robo3 proteins are expressed in the posterior midgut epithelium (data not shown; Robo1 is expressed in the proventriculus, explaining the detection of the Robo1 mRNA in dissected intestines). Robo2, on the other hand, was detected in esg-positive cells of the posterior midgut (Figure 1E), suggesting that Robo2 might be the ISC- and EB-specific receptor of Slit. To test this hypothesis, we used an inducible system to express a double-stranded RNA (dsRNA) construct directed against Robo2 (lea^{RNAi}, which efficiently knocks down Robo2 function; Tayler et al., 2004) specifically in ISCs and EBs (using the esg-Gal4 driver combined with a ubiquitously expressed temperature-sensitive Gal80 repressor, tubGal80^{ts}). This manipulation is sufficient to decrease the expression of Robo2 in esg-positive cells and in the intestine (Figures S1C and S1E) and to prevent the accumulation of the Slit protein at the periphery of these cells (Figures 1F and 1G). Conversely, overexpressing Robo2 (using a previously described Gal4-sensitive P element inserted into the *leak* locus, lea^{EP2582}) in ISCs and EBs is sufficient to increase the localization of the Slit protein to these cells without affecting its expression in EEs (Figures 1F and 1G). Altogether, these results indicate that the Slit ligand is secreted by EEs and may transmit a signal from EEs to ISCs and/or EBs through the Robo2 receptor.

The Robo2/Slit Pathway Regulates the Proportion of Endocrine Cells in the Intestinal Epithelium

To investigate the function of the Robo2-signaling pathway in the ISC lineage, we generated GFP-labeled ISC clones expressing the Robo2/lea^{RNAi} construct in the posterior midgut, using somatic recombination (mosaic analysis with a repressible cell marker [MARCM] method; Lee and Luo, 1999). Seven days after induction, lea^{RNAi}-expressing ISC clones showed normal growth compared to their wild-type counterparts, indicating that Robo2 is not required for ISC proliferation or self-renewal (Figure 2A). However, we found that the number of Prospero-positive cells in lea^{RNAi} clones is significantly higher than in control clones, suggesting that Robo2 may regulate the balance between EE and EC lineages (Figures 2A and S2A). We confirmed this *lea* loss of function phenotype by generating clones homozygous for the loss-of-function allele *lea*^{2}. Similar to what we observed using RNAi-mediated knockdown, we found that *robo2* homozygosity does not affect ISC proliferation or self-renewal but significantly increases the proportion of Prospero-positive cells in ISC clones (Figures 2B, S2B, and S2C). We further used the esg-Gal4^{ts} system to specifically manipulate the expression of Robo2 in all ISCs and EBs of adult flies. After 10 days of expression of the lea^{RNAi} construct in these cells, we observed an increased proportion of Prospero-positive cells in the intestinal epithelium (Figures 2C and 2D). Finally, we analyzed the composition of the epithelium of *lea*^{2} heterozygous mutants in 30-day-old animals (a time sufficient to allow at least one full turn-over of the female intestinal epithelium; Jiang et al., 2009) and found a significant accumulation of EEs in the midgut of these animals compared to wild-type controls (Figure 2E).

Based on these observations, we hypothesized that EE-derived Slit inhibits the formation of new EEs by promoting Robo2 activity in precursor cells. To test this idea, we first expressed three independent dsRNA constructs directed against Slit in adult flies using an inducible ubiquitous driver (actGal4GeneSwitch). Fifteen days after induction, we observed a significant increase in the proportion of EEs in the posterior midgut for all three RNAi constructs, similar to the phenotype induced by *lea* loss of function (Figure 2F). Next, to directly test the function of the Slit signal in the endocrine lineage, we identified an EE-specific Gal4 line that allows manipulating gene expression in these cells. We took advantage of a Gal4-containing P element inserted in the Amontillado gene (386YGal4), which encodes a protease required for the processing of peptide hormones in the fly intestine (Reiher et al., 2011). Similar to its activity in the larval intestine (Reiher et al., 2011), this driver is sufficient to specifically but weakly express upstream activating sequence (UAS)-driven GFP in most Prospero-positive and Slit-positive EEs in the adult intestinal epithelium (Figures S2D and S2E). We used this transgenic line to knock down Slit expression in EEs. Despite the weak activity of the 386YGal4 driver, 10 days after induction, we observed a small but significant increase in the proportion of Prospero-positive cells in the posterior midgut epithelium (Figure 2G).

Finally, we tested the effect of overexpressing Robo2/leak in ISC/EBs and overexpressing Slit in EEs, ECs, or ISC/EBs on tissue homeostasis. Surprisingly, we found that these manipulations do not affect the composition of the posterior midgut (Figures S2F and S2G). To confirm this result, we co-overexpressed Slit and Robo2/leak in ISC/EBs using the esgGal4 driver and observed no effect on the proportion of EEs in the posterior midgut (data not shown). These findings suggest that, whereas reduced Robo2/Slit signaling promotes EE production, ensuring replenishment of the EE pool when the amount of these cells falls under a critical threshold, endogenous Slit and Robo2 expression levels in the intestinal epithelium are sufficient and not limiting for the inhibition of excessive EE commitment.

Altogether, these results demonstrate that the Slit/Robo2-signaling pathway negatively influences the commitment of ISC daughter cells to the endocrine lineage. The origin of this signal is the EEs themselves, establishing a negative feedback loop and suggesting that ISCs constantly assess their immediate environment to control the destiny of their progeny and specifically replace missing EEs in the absence of a Slit signal.

The Endocrine Fate of Daughter Cells Is Established in ISCs Rather than EBs

To further refine our understanding of this signaling interaction, we asked whether the Slit/Robo2 signal functions on ISCs or EBs to control commitment to the EE lineage. ISCs can be distinguished from EBs by their differential expression of Dl (in ISCs) and Su(H)GBE reporters (in EBs; Ohlstein and Spradling, 2007). We knocked down Robo2 specifically in ISCs and EBs using the temperature-sensitive drivers DeltaGal4^{ts}

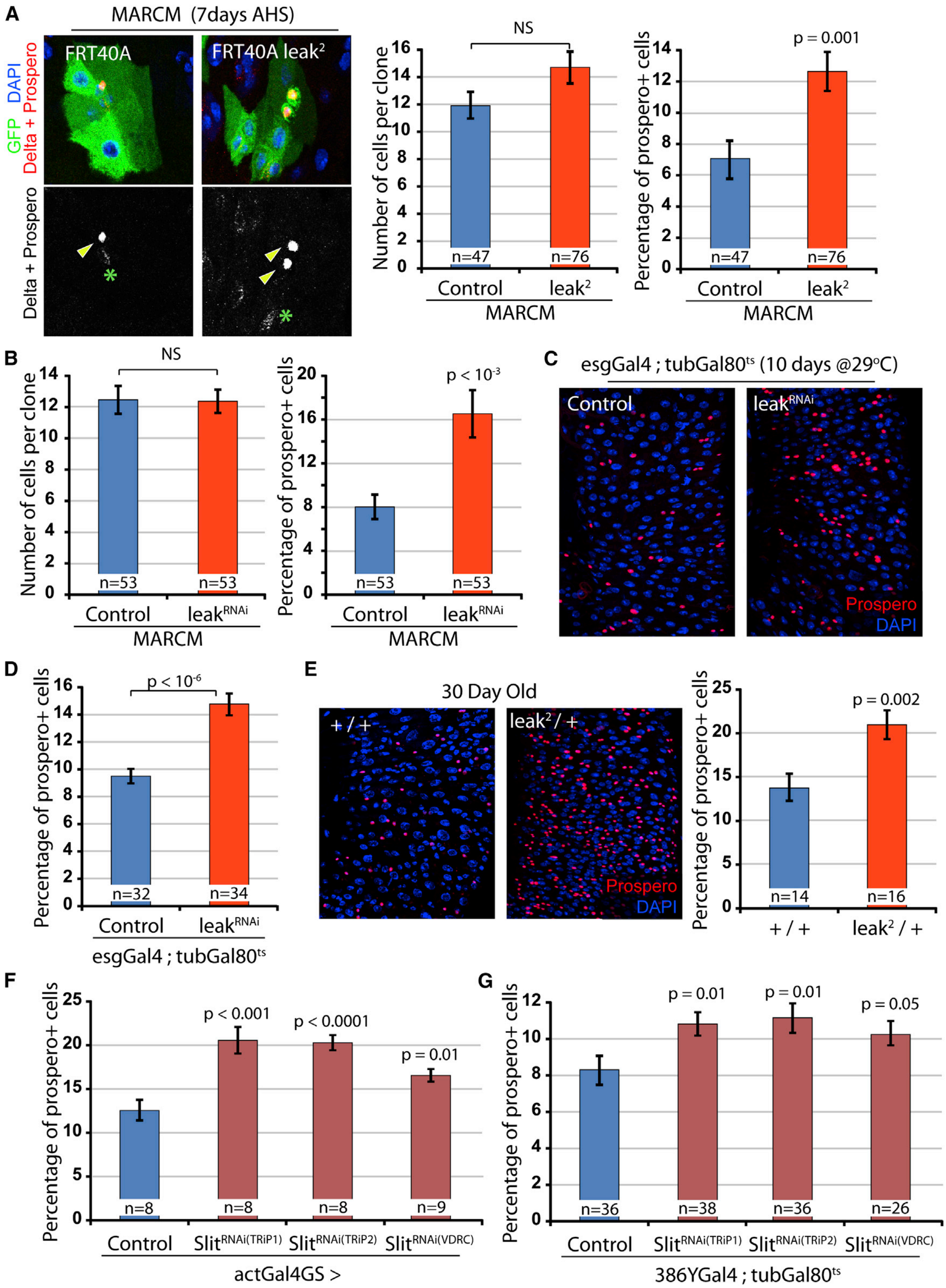

Figure 2. The Slit/Robo2 Pathway Regulates the Proportion of Endocrine Cells in the Intestinal Epithelium

(A and B) MARCM clones expressing a dsRNA directed against leak/Robo2 or homozygous for the mutant allele *lea*^{2} contain a greater proportion of Prospero-positive cells (arrowheads), 7 days after clone induction by heat shock (AHS), without affecting clone size. Confocal images show representative clones, Prospero labels EEs, and Delta marks ISCs (asterisks). NS, not significant.

(legend continued on next page)

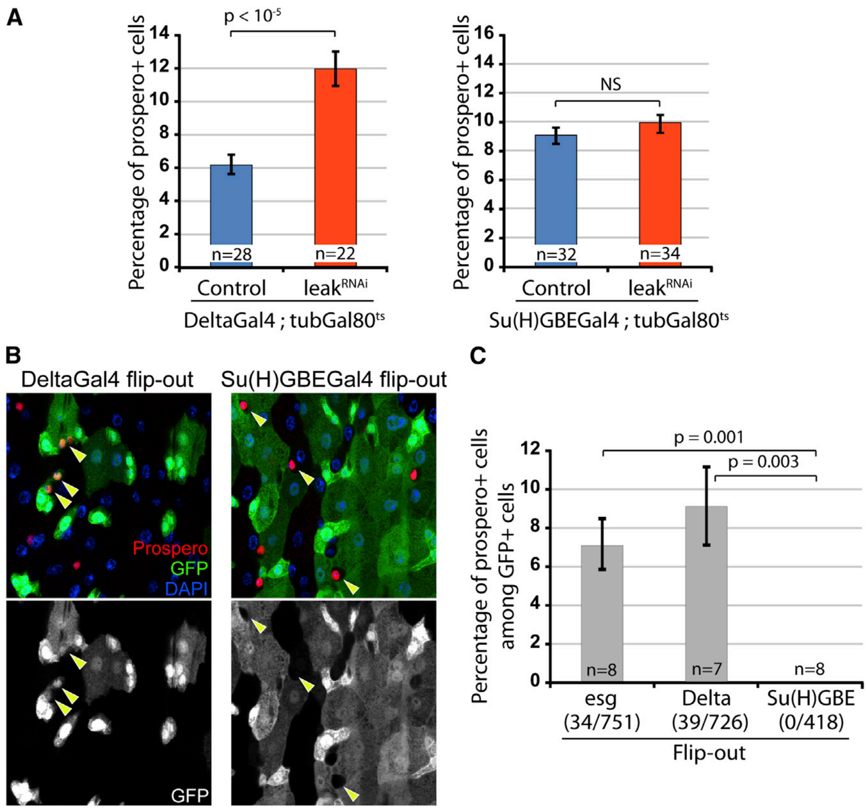

Figure 3. Commitment to the Endocrine Lineage Is Established in ISCs Rather than Enteroblasts

(A) Adult-specific knockdown of Robo2 in ISCs, using the temperature-sensitive DeltaGal4^{ts} drivers (10 days at 29°C), increases the proportion of Prospero-positive cells in the posterior midgut. Similar experiment using the EB-specific Su(H) GBEGal4^{ts} driver does not affect the composition of the intestinal epithelium.

(B and C) Flip-out lineage-tracing analysis of the progeny of esgGal4 (ISCs and EBs), DeltaGal4 (ISCs only), and Su(H)GBEGal4 (EBs only) expressing cells, 4 days after induction. GFP+Prospero double-positive cells (arrowheads) are found in the progeny of esgGal4- and DeltaGal4-positive cells but absent from the lineage of Su(H) GBEGal4-expressing cells. n indicates the number of guts analyzed; the numbers between parentheses represent the number of pros+ GFP+ cells/ total GFP+ cells.

p value from two-tailed Student's t test. Values are presented as average ± SEM.

and Su(H)GBEGal4^{ts} (Zeng et al., 2010). Similar to the results obtained using the esgGal4^{ts} driver, driving the leak^{RNAi} construct with the DeltaGal4^{ts} driver caused a significant increase of the proportion of EEs in the epithelium, whereas the composition of the intestine was not affected when leak^{RNAi} was expressed using Su(H)GBEGal4^{ts} (Figure 3A). Robo2 signaling thus seems to determine ISC daughter cell identity by acting in ISCs themselves rather than in Su(H)GBEGal4-expressing EBs.

Previous studies have proposed that two types of EBs are generated by ISCs: EC-committed EBs that express high levels of a reporter for Notch activity and EE-committed EBs (Ohlstein and Spradling, 2007). This lineage description was supported by genetic evidence demonstrating that loss of Delta/Notch function in ISCs impairs EC differentiation while promoting the specification of EEs (Micchelli and Perrimon, 2006; Ohlstein and Spradling, 2006, 2007; Perdigoto et al., 2011). So far, markers for the EE-committed EB population have not been described, and lineage tracing experiments have not yet definitively established the existence of these cells. To test this model, we therefore first analyzed the composition of the progeny of esgGal4- (ISCs and EBs), deltaGal4- (only ISCs; Zeng et al., 2010) or Su(H) GBEGal4 (only EBs)-expressing cells, using an adult-specific lineage-tracing strategy in which heritable expression of GFP was induced by recombination initiated from a UAS-linked Flippase. We found that EEs represent 6%–10% of the progeny of ISCs (Figures 3B and 3C; using both esgGal4 and DeltaGal4), a proportion similar to the one found in the whole intestinal epithelium. Strikingly, however, we found that Prospero-expressing EEs are absent from the progeny of Su(H)GBEGal4-expressing cells. This demonstrates that EBs (defined as ISC daughter cells that show high levels of Notch signaling activity) are not multipotent, as they do not have the capacity to generate EEs but are rather EC-committed precursors prior to their terminal differentiation.

Prospero Expression in ISCs Is Required for EE Commitment and Influenced by Robo2

In addition to clarifying the intestinal lineage, these results raise two possibilities regarding the commitment of intestinal progenitors: cell specification to the EC or EE lineage may occur before cell division and ISCs give rise to already distinct daughter cells,

(C and D) Adult-specific knockdown of Robo2 in ISCs and EBs, using the temperature-sensitive esgGal4^{ts} (10 days at 29°C), causes an accumulation of Prospero-positive cells in the intestinal epithelium.

(E) Quantification of the proportion of Prospero-positive cells in 30-day-old *lea*^{2} heterozygous and control flies shows an accumulation of EEs in the intestine of mutant animals.

(F and G) Ubiquitous knockdown of Slit (act5cGal4GeneSwitch; 15 days treatment with RU486) is sufficient to induce an increase in the proportion of EEs in the intestinal epithelium. Similar phenotype is observed when Slit^{RNAi} constructs are specifically expressed in EE, using the temperature-sensitive 386YGal4^{ts} driver. Three independent RNAi constructs were tested.

n represents the number of clones analyzed in (A) and (B) and the number of posterior midguts observed in (C)–(G). p value from two-tailed Student's t test. Values are presented as average ± SEM. See also Figure S2.

or the specification may take place in already formed ISC/precursor pairs, in which the level of expression of Dl in ISCs is regulated to activate or not the Notch signaling pathway in the neighboring cell. Distinguishing between these two models is essential to understand the role of Robo2 in the cell-fate decision. Importantly, we and others have observed that, when Delta/Notch signaling is impaired in ISCs (a genetic manipulation that causes a dramatic accumulation of EEs in the intestinal epithelium; Micchelli and Perrimon, 2006; Ohlstein and Spradling, 2006, 2007), the EE marker Prospero can be detected in a subset of esg-positive cells (Biteau et al., 2008; Liu et al., 2010; Micchelli and Perrimon, 2006), including in mitotic cells (Figure S3A). Therefore, we tested the notion that Prospero-positive ISCs may exist in wild-type animals. To this end, we reassessed the expression pattern of Prospero in the epithelium of wild-type animals and found that around 6% of the cells positive for the mitotic marker phospho-histone H3 (pH3) also express Prospero (Figures 4A and 4B), suggesting that these cells may have adopted an endocrine fate. Next, using the esgGal4 and esgLacZ reporters, we found that these pH3+pros+ cells also express the *escargot* ISC and EB marker (Figures 4C and S3B). Finally, using immunocytochemistry, we confirmed that both the Delta and Prospero proteins are detected in this population of mitotic cells (Figures 4D and S3C), demonstrating that these cells are EE-committed dividing progenitors and not dividing terminally differentiated EEs.

Our previous results suggest that Prospero expression in ISCs, prior to cell division, promotes EE commitment. To test this model, we used the esgGal4^{ts}, deltaGal4^{ts}, and Su(H) GBEGal4^{ts} drivers to knock down Prospero in ISCs and/or EBs. We found that expression of Prospero^{RNAi} for 10 days in ISCs (esgGal4+ and DeltaGal4+ cells), but not in Su(H)GBE+ cells, significantly reduced the proportion of EEs in the intestine (Figure 3F), confirming that Prospero expression in ISCs themselves is required for optimal maintenance of the EE lineage.

Because we find that Slit/Robo2 signaling negatively influences the production of EEs, we assessed the influence of Robo2 on the expression of Prospero in mitotic ISCs and found that the proportion of pH3+pros+ cells is greatly augmented when Robo2 expression is knocked down (Figure 4E), mirroring the increase in EEs in the progeny of these mutant ISCs. Importantly, Prospero knockdown suppresses this Robo2 loss-of-function phenotype (Figure 4F), confirming that the proposed Robo2-mediated cell fate decision mechanism acts upstream of Prospero expression in ISCs.

Robo2 Regulates Lineage Specification Upstream and Independently of Notch Signaling

Our data support a model in which Slit/Robo2 controls cell fate decisions in the ISC lineage by regulating the specification of ISCs into Prospero-expressing EE precursors before or during mitosis. Interestingly, we found that manipulating the activity of Robo2 in ISCs does not affect the phenotype generated by expression of Notch^{RNAi} (in which the formation of EC-committed EBs is specifically inhibited; Figure S4A). In addition, we found no evidence that loss of Robo2 affects Delta expression in ISCs (data not shown). Finally, the activation of the Notch pathway is sufficient to promote differentiation independently of Robo2 signaling (Figure S4B). This supports the idea that Robo2 acts upstream and independently of the activation of the Notch signaling pathway, regulating lineage commitment in ISCs, whereas Notch specifically controls differentiation of daughter cells into the EC fate. In this model, the absence of Notch signaling results in default commitment of ISC daughter cells into an EE fate, and lineage commitment thus becomes independent of Robo2/Slit signaling, because EC differentiation is impaired (Figures S4C and S4D).

It is interesting to note that the intensity of the Slit signal is integrated by ISCs to generate an all-or-nothing response: above a defined Slit threshold, Prospero is expressed by around 6% of mitotic ISCs, whereas below this level, 15%–20% of ISCs express Prospero, and no intermediate expression of Prospero can be detected. Further studies will be required to characterize the signaling cascade that controls Prospero expression downstream of the Robo2 receptor in ISCs.

Robo4 has recently been identified as a regulator of hematopoietic stem cell homing in mice (Shibata et al., 2009; Smith-Berdan et al., 2011). In addition, proteins of the Slit and Robo families have been suggested to act as tumor suppressors and be directly involved in the tumorigenesis process (Biankin et al., 2012; Legg et al., 2008; Marlow et al., 2008; Zhou et al., 2011). Our study identifies a mechanism by which differentiated cells engage this pathway to directly regulate stem cell function and lineage commitment. A role for Slit/Robo signaling in the control of fate decisions in mammalian normal or cancer stem cell lineages has not yet been tested. However, based on the conservation of mechanisms that control *Drosophila* ISC self-renewal and differentiation (Biteau et al., 2011; Casali and Batlle, 2009; Jiang and Edgar, 2012; Wang and Hou, 2010), it can be anticipated that this feedback control of stem cell fate decisions through Slit/Robo signaling also controls adult tissue homeostasis in higher organisms.

EXPERIMENTAL PROCEDURES

Drosophila Stocks and Culture

The following strains were obtained from the Bloomington *Drosophila* Stock Center: OregonR, *w^{1118}*, *lea*^{2}, *lea*^{EP2582}, UAS-lea^{RNAi}, UAS-Slit, *pros*^{38} (pros-GFP), slit^{PZ05248}, esg^{k00606}, P{GawB}386Y, UAS-Flp (no. 5254), and act > y > Gal4, UAS-GFP (no. 4411), UAS-mCherry. UAS-Slit$^{RNAi(TRiP1)}$ and UAS-Slit$^{RNAi(TRiP2)}$ are from the Transgenic RNAi Project, stocks JF01228 and JF01229. UAS-Slit$^{RNAi(VDRC)}$ and UAS-Prospero^{RNAi} were obtained from the Vienna *Drosophila* RNAi Center (transformant ID 20210 and 101477, respectively). The line esg-Gal4^{NP5130} was kindly provided by S. Hayashi, DeltaGal4 and Su(H)GBEGal4 by S. Hou, UAS-Notch^{RNAi} by N. Perrimon, UAS-Notch^{intra} by M. Rand, actin5cGal4Geneswitch(255) by J. Towers, and NP1Gal4 by D. Ferrandon.

The UAS-lea^{RNAi}, UAS-Slit$^{RNAi(VDRC)}$, and UAS-Pros^{RNAi} were validated and successfully used in previous studies (Brierley et al., 2009; Neumüller et al., 2011; Tayler et al., 2004).

Flies were raised on standard yeast and molasses-based food, at 25°C and 65% humidity, on a 12 hr light/dark cycle, unless otherwise indicated.

Conditional Expression of UAS-Linked Transgenes

The TARGET system was used to conditionally express UAS-linked transgenes in ISCs and/or EBs. The esgGal4, DeltaGal4, and Su(H)GBEGal4 drivers were combined with a ubiquitously expressed temperature-sensitive Gal80 inhibitor (tub-Gal80^{ts}). Crosses and flies were kept at 18°C (permissive temperature), and 3- to 5-day-old adults were then shifted to 29°C to allow expression of the transgenes.

For ubiquitous expression using the actin5cGal4GeneSwitch, adult flies were fed RU486 as described before (Biteau et al., 2010).

OPEN ACCESS
CellPress

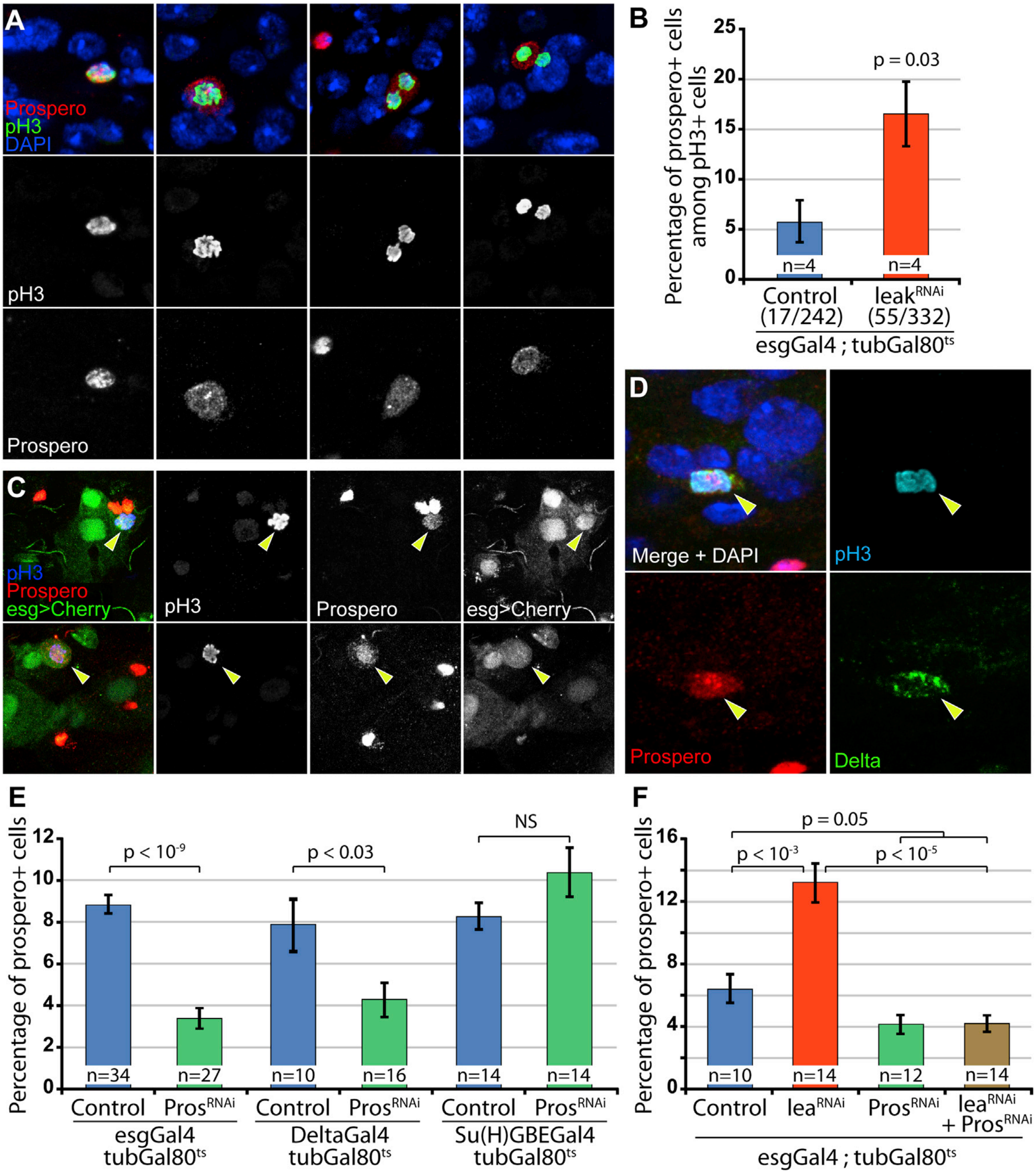

Figure 4. Prospero Expression in ISCs Is Regulated by the Robo2 Pathway

(A) Representative images of pros+pH3 double-positive cells in the posterior midgut of wild-type flies.

(B) Quantification of the proportion of pros+ cells among dividing pH3+-positive cells in control flies or after knocking down Robo2 expression in esg-positive cells for 10 days. n represents the number of independent experiments; the numbers indicated below the genotypes represent the total number of pH3+ cells counted.

(C) Representative images of esgGal4 > mCherry pH3+ pros+ cells.

(D) Representative image of a mitotic cell expressing both the Delta and Prospero proteins (see Figure S3C for additional examples).

(E) Adult-specific knockdown of Prospero in ISCs leads to a decrease in the proportion of EEs in the intestine.

(F) Knockdown of Prospero in esg-positive cells suppresses the increased proportion of EEs induced by lea^{RNAi} expression.

n indicates the number of guts analyzed in (B), (E), and (F). p value from two-tailed Student's t test. Values are presented as average ± SEM. See also Figure S3.

MARCM Clones and Flip-Out Lineage Tracing

Positively marked clones were generated by somatic recombination using the following MARCM stock: hsFlp;FRT40A tub-Gal80;tub-Gal4,UAS-GFP (gift from B. Ohlstein). Virgins were crossed to the following lines: FRT40A *lea2* or FRT40A;UAS-lea^{RNAi}. Three- to five-day-old mated female flies were heat shocked for 45 min at 37°C to induce somatic recombination.

Flies were transferred to 25°C, and clones were observed 7 days after induction.

For Flip-out lineage-tracing analysis, the following genotypes were used: UAS-Flp/+; esg-Gal4,UAS-GFP/act5c-FRT-y-FRT-Gal4,UAS-GFP; tubulin-Gal80^{ts}/+, UAS-Flp/+; Su(H)GBE-Gal4,UAS-GFP/act5c-FRT-y-FRT-Gal4, UAS-GFP; tubulin-Gal80^{ts}/+, and UAS-Flp/+; act5c-FRT-y-FRT-Gal4,UAS-GFP/+; Delta-Gal4,UAS-GFP/tubulin-Gal80^{ts}.

Crosses were set up at 18°C. Then, 3- to 5-day-old females were heat shocked at 37°C for 30 min and transferred to 29°C to induce the expression of UAS-driven Flippase and permanently label ISCs and/or EBs and their progeny. The composition of the lineages was analyzed 4 days after labeling.

Immunocytochemistry and Microscopy

Fly intestines were dissected in PBS and fixed at room temperature for 45 min in 100 mM glutamic acid, 25 mM KCl, 20 mM $MgSO_4$, 4 mM sodium phosphate, 1 mM $MgCl_2$, and 4% formaldehyde. All subsequent incubations were done in PBS, 0.5% BSA, and 0.1% Triton X-100 at 4°C.

The following primary antibodies were obtained from the Developmental Studies Hybridoma Bank: mouse anti-slit, anti-Delta, anti-Prospero, anti-Armadillo, and anti-β-galactosidase and used 1:50, 1:100, 1:250, 1:100, and 1:500, respectively. Rabbit anti-β-galactosidase is from Cappel and used 1:1,000; rabbit anti-pH3 from Upstate, 1:1,000. The anti-Robo2 was obtained from B. Dickson and used 1:50. The rat anti-Delta was obtained from M. Rand and used 1:200. Fluorescent secondary antibodies were obtained from Jackson Immunoresearch. Hoechst was used to stain DNA.

Confocal images were collected using a Leica SP5 confocal system and processed using the Leica software and Adobe Photoshop CS5.

To quantify the intensity of the slit immunocytochemistry in Figure 1G, the mean pixel intensity for the appropriate color channel of EEs and ISCs was measured using the Adobe Photoshop CS5 software. The intensity of each ISC was normalized to the intensity of the closest EE to take into account differences in staining between intestines and experiments.

Phenotype Analysis

For clonal studies, only isolated clones that can be identified with confidence were included in the analysis of clone size and composition.

For all experiments, the data are represented as average ± SEM. All p values are calculated using unpaired two-tailed Student's t test.

SUPPLEMENTAL INFORMATION

Supplemental Information includes Supplemental Experimental Procedures and four figures and can be found with this article online at http://dx.doi.org/10.1016/j.celrep.2014.05.024.

ACKNOWLEDGMENTS

We thank M. Nuzzo and the University of Rochester Genomics Research Center for technical assistance as well as M. Rand, J. Tower, B. Dickson, D. Ferrandon, S. Hayashi, S. Hou, N. Perrimon, the Bloomington Drosophila Stock Center, the Vienna Drosophila RNAi Center, and the Developmental Studies Hybridoma Bank for providing essential reagents. This work was supported by an Ellison Medical Foundation/AFAR postdoctoral award and a New Scholar in Aging Research from the Ellison Medical Foundation (AG-NS-0990-13) to B.B. and by grants from the National Institute on General Medical Sciences (NIH RO1 GM100196) and the Ellison Medical Foundation (AG-SS-2224-08) to H.J.

Received: March 19, 2014
Revised: March 21, 2014
Accepted: May 12, 2014
Published: June 12, 2014

REFERENCES

Amcheslavsky, A., Jiang, J., and Ip, Y.T. (2009). Tissue damage-induced intestinal stem cell division in Drosophila. Cell Stem Cell *4*, 49–61.

Beck, B., and Blanpain, C. (2012). Mechanisms regulating epidermal stem cells. EMBO J. *31*, 2067–2075.

Biankin, A.V., Waddell, N., Kassahn, K.S., Gingras, M.C., Muthuswamy, L.B., Johns, A.L., Miller, D.K., Wilson, P.J., Patch, A.M., Wu, J., et al.; Australian Pancreatic Cancer Genome Initiative (2012). Pancreatic cancer genomes reveal aberrations in axon guidance pathway genes. Nature *491*, 399–405.

Biteau, B., Hochmuth, C.E., and Jasper, H. (2008). JNK activity in somatic stem cells causes loss of tissue homeostasis in the aging Drosophila gut. Cell Stem Cell *3*, 442–455.

Biteau, B., Karpac, J., Supoyo, S., Degennaro, M., Lehmann, R., and Jasper, H. (2010). Lifespan extension by preserving proliferative homeostasis in Drosophila. PLoS Genet. *6*, e1001159.

Biteau, B., Hochmuth, C.E., and Jasper, H. (2011). Maintaining tissue homeostasis: dynamic control of somatic stem cell activity. Cell Stem Cell *9*, 402–411.

Brierley, D.J., Blanc, E., Reddy, O.V., Vijayraghavan, K., and Williams, D.W. (2009). Dendritic targeting in the leg neuropil of Drosophila: the role of midline signalling molecules in generating a myotopic map. PLoS Biol. *7*, e1000199.

Buchon, N., Broderick, N.A., Chakrabarti, S., and Lemaitre, B. (2009). Invasive and indigenous microbiota impact intestinal stem cell activity through multiple pathways in Drosophila. Genes Dev. *23*, 2333–2344.

Casali, A., and Batlle, E. (2009). Intestinal stem cells in mammals and Drosophila. Cell Stem Cell *4*, 124–127.

Chatterjee, M., and Ip, Y.T. (2009). Pathogenic stimulation of intestinal stem cell response in Drosophila. J. Cell. Physiol. *220*, 664–671.

Cronin, S.J., Nehme, N.T., Limmer, S., Liegeois, S., Pospisilik, J.A., Schramek, D., Leibbrandt, A., Simoes, Rde.M., Gruber, S., Puc, U., et al. (2009). Genome-wide RNAi screen identifies genes involved in intestinal pathogenic bacterial infection. Science *325*, 340–343.

de Navascués, J., Perdigoto, C.N., Bian, Y., Schneider, M.H., Bardin, A.J., Martínez-Arias, A., and Simons, B.D. (2012). Drosophila midgut homeostasis involves neutral competition between symmetrically dividing intestinal stem cells. EMBO J. *31*, 2473–2485.

Jiang, H., and Edgar, B.A. (2012). Intestinal stem cell function in Drosophila and mice. Curr. Opin. Genet. Dev. *22*, 354–360.

Jiang, H., Patel, P.H., Kohlmaier, A., Grenley, M.O., McEwen, D.G., and Edgar, B.A. (2009). Cytokine/Jak/Stat signaling mediates regeneration and homeostasis in the Drosophila midgut. Cell *137*, 1343–1355.

Kidd, T., Brose, K., Mitchell, K.J., Fetter, R.D., Tessier-Lavigne, M., Goodman, C.S., and Tear, G. (1998). Roundabout controls axon crossing of the CNS midline and defines a novel subfamily of evolutionarily conserved guidance receptors. Cell *92*, 205–215.

Lee, T., and Luo, L. (1999). Mosaic analysis with a repressible cell marker for studies of gene function in neuronal morphogenesis. Neuron *22*, 451–461.

Legg, J.A., Herbert, J.M., Clissold, P., and Bicknell, R. (2008). Slits and Roundabouts in cancer, tumour angiogenesis and endothelial cell migration. Angiogenesis *11*, 13–21.

Liu, W., Singh, S.R., and Hou, S.X. (2010). JAK-STAT is restrained by Notch to control cell proliferation of the Drosophila intestinal stem cells. J. Cell. Biochem. *109*, 992–999.

Marlow, R., Strickland, P., Lee, J.S., Wu, X., Pebenito, M., Binnewies, M., Le, E.K., Moran, A., Macias, H., Cardiff, R.D., et al. (2008). SLITs suppress tumor growth in vivo by silencing Sdf1/Cxcr4 within breast epithelium. Cancer Res. *68*, 7819–7827.

Micchelli, C.A., and Perrimon, N. (2006). Evidence that stem cells reside in the adult Drosophila midgut epithelium. Nature *439*, 475–479.

Neumüller, R.A., Richter, C., Fischer, A., Novatchkova, M., Neumüller, K.G., and Knoblich, J.A. (2011). Genome-wide analysis of self-renewal in Drosophila neural stem cells by transgenic RNAi. Cell Stem Cell *8*, 580–593.

Ohlstein, B., and Spradling, A. (2006). The adult Drosophila posterior midgut is maintained by pluripotent stem cells. Nature *439*, 470–474.

Ohlstein, B., and Spradling, A. (2007). Multipotent Drosophila intestinal stem cells specify daughter cell fates by differential notch signaling. Science *315*, 988–992.

Perdigoto, C.N., Schweisguth, F., and Bardin, A.J. (2011). Distinct levels of Notch activity for commitment and terminal differentiation of stem cells in the adult fly intestine. Development *138*, 4585–4595.

Rajagopalan, S., Nicolas, E., Vivancos, V., Berger, J., and Dickson, B.J. (2000). Crossing the midline: roles and regulation of Robo receptors. Neuron *28*, 767–777.

Reiher, W., Shirras, C., Kahnt, J., Baumeister, S., Isaac, R.E., and Wegener, C. (2011). Peptidomics and peptide hormone processing in the Drosophila midgut. J. Proteome Res. *10*, 1881–1892.

Rock, J.R., and Hogan, B.L. (2011). Epithelial progenitor cells in lung development, maintenance, repair, and disease. Annu. Rev. Cell Dev. Biol. *27*, 493–512.

Shibata, F., Goto-Koshino, Y., Morikawa, Y., Komori, T., Ito, M., Fukuchi, Y., Houchins, J.P., Tsang, M., Li, D.Y., Kitamura, T., and Nakajima, H. (2009). Roundabout 4 is expressed on hematopoietic stem cells and potentially involved in the niche-mediated regulation of the side population phenotype. Stem Cells *27*, 183–190.

Simpson, J.H., Bland, K.S., Fetter, R.D., and Goodman, C.S. (2000). Short-range and long-range guidance by Slit and its Robo receptors: a combinatorial code of Robo receptors controls lateral position. Cell *103*, 1019–1032.

Smith-Berdan, S., Nguyen, A., Hassanein, D., Zimmer, M., Ugarte, F., Ciriza, J., Li, D., García-Ojeda, M.E., Hinck, L., and Forsberg, E.C. (2011). Robo4 cooperates with CXCR4 to specify hematopoietic stem cell localization to bone marrow niches. Cell Stem Cell *8*, 72–83.

Tayler, T.D., Robichaux, M.B., and Garrity, P.A. (2004). Compartmentalization of visual centers in the Drosophila brain requires Slit and Robo proteins. Development *131*, 5935–5945.

Wang, P., and Hou, S.X. (2010). Regulation of intestinal stem cells in mammals and Drosophila. J. Cell. Physiol. *222*, 33–37.

Yeung, T.M., Chia, L.A., Kosinski, C.M., and Kuo, C.J. (2011). Regulation of self-renewal and differentiation by the intestinal stem cell niche. Cell. Mol. Life Sci. *68*, 2513–2523.

Ypsilanti, A.R., Zagar, Y., and Chédotal, A. (2010). Moving away from the midline: new developments for Slit and Robo. Development *137*, 1939–1952.

Zeng, X., Chauhan, C., and Hou, S.X. (2010). Characterization of midgut stem cell- and enteroblast-specific Gal4 lines in Drosophila. Genesis *48*, 607–611.

Zhou, W.J., Geng, Z.H., Chi, S., Zhang, W., Niu, X.F., Lan, S.J., Ma, L., Yang, X., Wang, L.J., Ding, Y.Q., and Geng, J.G. (2011). Slit-Robo signaling induces malignant transformation through Hakai-mediated E-cadherin degradation during colorectal epithelial cell carcinogenesis. Cell Res. *21*, 609–626.